

# Bayesian Broadband Passive Sonar Tracking

Ryan J. Pirkl, Bryan A. Yocom, and Jason M. Aughenbaugh

Applied Research Laboratories  
 The University of Texas at Austin  
 Austin, TX 78713-8029  
 Email: {rpirkl, jason}@arlut.utexas.edu

**Abstract**—We present a Bayesian tracker for broadband passive sonar. The Bayesian formulation in Cartesian coordinates facilitates multi-sensor fusion of a distributed field of receivers. The likelihood functions used in the tracker are formulated so as to leverage *a priori* knowledge about the signal-of-interest’s bandwidth and spectral mask when available. The use of *a priori* knowledge about the signal enables substantial gains in the tracker’s detection and localization performance, even when this knowledge is approximate.

## I. INTRODUCTION

Sub-band energy detection schemes (e.g., sub-band peak energy detector [SPED] and sub-band extrema energy detector [SEED]) have long been the de facto standard for processing broadband passive sonar measurements from a single sensor [1], [2]. However, these approaches are ill-suited for data-fusion-type applications wherein measurements are available from multiple distributed sensors. In contrast, likelihood functions combined with a Bayesian tracker provide a natural paradigm for multi-sensor data fusion.

For broadband sources, the likelihood function is typically formulated in terms of the total power within a given conventional beamformer (CBF) beam after integrating over the entire measurement bandwidth [3], [4]. However, the likelihood function may alternatively be derived based on the statistics of the raw signals observed at the outputs of the array elements [5]. For a single signal of interest, the use of the raw signal allows the likelihood function to implicitly leverage the interference and noise rejection capabilities of adaptive beamforming as was demonstrated in [6] for narrowband signals and [7] for broadband signals.

Here, we extend the likelihood formulation described in [6], [8] for use with broadband signals. We describe two different approaches to marginalizing the broadband likelihood ratios. One approach is applicable when one has no *a priori* knowledge of the signal’s spectral mask; the other approach leverages *a priori* knowledge of the signal’s spectral mask to significantly improve tracking performance. Simulation results obtained by use of a 2-D Cartesian-based position-velocity Bayesian tracker reveal that this latter approach is robust to errors in the assumed spectral mask of the signal.

We begin by describing the signal model in Section II. Narrowband and broadband single-signal log-likelihood ratios (SSLRs) are presented in Section III. Section IV describes the process for estimating various signal and noise parameters required to use the SSLRs. We consider two different

approaches to estimating the signal parameters depending on the available *a priori* knowledge of the signal of interest. In Section V, we assess the performance of a Bayesian tracker for a broadband signal with a range of potential bandwidths and different degrees of *a priori* knowledge of the signal (e.g., known/unknown bandwidth and spectral mask). Conclusions are presented in Section VI.

## II. SIGNAL MODEL

At a frequency  $f$ , the  $k$ th  $T$ -second snapshot of the output of an  $N$  element array of omnidirectional sensors in the presence of  $M + 1$  uncorrelated sources and ambient noise may be described by an  $N$ -element column vector  $\mathbf{x}$  given by

$$\mathbf{x}_k(f) = \sum_{m=0}^M s_{k,m}(f) \mathbf{v}(\phi_m, f) + \mathbf{n}_k(f), \quad (1)$$

where  $s_{k,m}(f)$  is the signal due to the  $m$ th source during snapshot  $k$ ,  $\mathbf{v}$  is the array steering vector,  $\phi_m$  denotes the direction of arrival of the  $m$ th source’s signal in azimuth during snapshot  $k$ , and  $\mathbf{n}_k(f)$  is the ambient noise during snapshot  $k$ . Here,  $k \in \{1, 2, \dots, K\}$ ,  $m \in \{0, 1, \dots, M\}$ , and we assume  $M$  is known. For simplicity, we assume that  $\phi_m$  is effectively constant over  $K$  snapshots. We also assume all sources are in the far-field of the array whereby the signals impinging on the array may be modeled as plane waves. The array steering vector  $\mathbf{v}(\phi, f)$  is an  $N$ -element column vector given by

$$\mathbf{v}(\phi, f) = [ e^{j\mathbf{k}(\phi, f) \cdot \mathbf{r}_1} \quad \dots \quad e^{j\mathbf{k}(\phi, f) \cdot \mathbf{r}_N} ]^T \quad (2)$$

for some direction of arrival  $\phi$ . In (2),  $\mathbf{r}_n$ ,  $n \in \{1, 2, \dots, N\}$  denotes the position of the  $n$ th array element, and  $\mathbf{k}$  is the wavevector given by

$$\mathbf{k}(\phi, f) = \frac{2\pi f}{c} \hat{\mathbf{k}}(\phi), \quad (3)$$

where  $c$  is the speed of sound and  $\hat{\mathbf{k}}(\phi)$  is a unit vector in the direction  $\phi$ . The element-level sample covariance matrix is given by

$$\mathbf{C}_{\mathbf{x}}(f) = \frac{1}{K} \sum_{k=1}^K \mathbf{x}_k(f) \mathbf{x}_k^H(f), \quad (4)$$

whereby the covariance matrix is estimated from  $K$  snapshots and  $(\cdot)^H$  denotes the conjugate transpose.

We assume  $s_{k,m}(f)$  and  $\mathbf{n}_k(f)$  for all  $k, m$  may be described by uncorrelated circular complex Gaussian random processes that are wide-sense stationary over the  $K$  snapshots. Then, the covariance matrix of  $\mathbf{x}_k(f)$  is

$$\begin{aligned} \mathbf{R}_{\mathbf{x}}(\mathbf{s}, f) &= E\{\mathbf{x}_k(f)\mathbf{x}_k^H(f)\} \\ &= \sum_{m=0}^M P_m p_m(f) \mathbf{v}(\phi_m, f) \mathbf{v}^H(\phi_m, f) + \mathbf{R}_{\mathbf{n}}(f), \end{aligned} \quad (5)$$

where  $P_m$  is the total power of the  $m$ th source's signal,  $p_m(f)$  is the signal's spectral mask defined such that  $P_m p_m(f)$  is the corresponding power-spectral density, and  $\mathbf{R}_{\mathbf{n}}$  is the covariance matrix of the noise  $\mathbf{n}_k$  as given by

$$\mathbf{R}_{\mathbf{n}}(f) = E\{\mathbf{n}_k(f)\mathbf{n}_k^H(f)\}. \quad (6)$$

### III. SINGLE-SIGNAL LOG-LIKELIHOOD RATIO

We consider the SLLR as described in [6], [8]. The SLLR is the marginalization of the log-likelihood ratio, given by

$$\begin{aligned} \log L(\mathbf{X}|\mathbf{s}) &= \\ &= \sum_{q=1}^Q -K [\log |\mathbf{R}_{\mathbf{x}}(\mathbf{s}, f_q)| + \text{tr}(\mathbf{R}_{\mathbf{x}}^{-1}(\mathbf{s}, f_q) \mathbf{C}_{\mathbf{x}}(f_q))], \end{aligned} \quad (7)$$

such that it depends only on the signal-of-interest's direction-of-arrival. In (7),  $\mathbf{s} = \{P_m, \phi_m, \mathbf{R}_{\mathbf{n}}\}_{m=0}^M$  is the set of all considered state parameters and  $\mathbf{X} = \{\mathbf{x}_k\}_{k=1}^K$  is the set of  $K$  snapshots.

#### A. Narrowband

At a single frequency, the SLLR for the  $m'$ th source is

$$\begin{aligned} \log L_{m'}(\mathbf{X}(f)|\phi_{m'}) &= K \left[ -\log \left( 1 + \frac{P_{m'} p_{m'}(f)}{\nu_{m'}(\phi_{m'})} \right) \right. \\ &\quad \left. + \left( \frac{\frac{P_{m'} p_{m'}(f)}{\nu_{m'}(\phi_{m'}, f)}}{1 + \frac{P_{m'} p_{m'}(f)}{\nu_{m'}(\phi_{m'}, f)}} \right) \frac{P_{\text{MVDR}, m'}(\phi_{m'}, f)}{\nu_{m'}(\phi_{m'}, f)} \right] \end{aligned} \quad (8)$$

as presented in [6]. In (8),  $P_{\text{MVDR}, m'}$  is the minimum variance distortionless response (MVDR) power versus look angle as given by

$$P_{\text{MVDR}, m'}(\phi, f) = \mathbf{w}_{m'}^H(\phi, f) \mathbf{C}_{\mathbf{x}}(f) \mathbf{w}_{m'}(\phi, f), \quad (9)$$

$\nu_{m'}(\phi, f)$  is the average received noise-plus-interference with respect to the  $m'$ th source as given by

$$\nu_{m'}(\phi, f) = \mathbf{w}_{m'}^H(\phi, f) \mathbf{R}_{n+i, m'}(f) \mathbf{w}_{m'}(\phi, f), \quad (10)$$

$\mathbf{w}_{m'}$  is the MVDR beamformer weights given by

$$\mathbf{w}_{m'}(\phi, f) = \frac{\mathbf{R}_{n+i, m'}^{-1}(f) \mathbf{v}(\phi, f)}{\mathbf{v}^H(\phi, f) \mathbf{R}_{n+i, m'}^{-1}(f) \mathbf{v}(\phi, f)}, \quad (11)$$

and  $\mathbf{R}_{n+i, m'}(f)$  is the combined noise-plus-interference covariance matrix with respect to the  $m'$ th source as given by

$$\begin{aligned} \mathbf{R}_{n+i, m'}(\mathbf{s}, f) &= \\ &= \sum_{\substack{m=0 \\ m \neq m'}}^M P_m p_m(f) \mathbf{v}(\phi_m, f) \mathbf{v}^H(\phi_m, f) + \mathbf{R}_{\mathbf{n}}(f). \end{aligned} \quad (12)$$

Note that the computation of  $\mathbf{R}_{n+i, m'}^{-1}$  in (11) can be unstable due to the matrix's potentially large condition number. A regularized approach to computing the inverse is described in [9].

#### B. Broadband

When the signal of interest spans multiple frequencies  $f_q$  with  $q \in \{1, 2, \dots, Q\}$ , we may sum (8) over all  $f_q$  under the assumption that the signal and noise at different  $f_q$  are uncorrelated. This is a reasonable assumption for many types of signals that may be modeled as random processes. Using this assumption, the broadband single-signal log-likelihood ratio takes the form

$$\log L_{m'}(\mathbf{X}|\phi_{m'}) = \sum_{q=1}^Q \log L_{m'}(\mathbf{X}(f_q)|\phi_{m'}). \quad (13)$$

The summation in (13) is nominally over the frequency band of interest, but it may also be taken across the entire measurement band at the cost of reduced detection and tracking performance. This may be appropriate when the bandwidth and/or center frequency of the  $m'$ th signal is unknown.

### IV. MARGINALIZATION OF THE BROADBAND SINGLE-SIGNAL LIKELIHOOD RATIO

Evaluation of the broadband SLLRs requires estimates of the interfering sources' parameters  $\phi_m$ ,  $P_m$ , and  $p_m(f)$  for  $m \neq m'$ ; the noise covariance matrix  $\mathbf{R}_{\mathbf{n}}(f)$ ; and the signal-of-interest's power  $P_{m'}$  and spectral mask  $p_{m'}(f)$ . In this section, we discuss how these parameters may be estimated.

#### A. Noise Estimation

We assume the noise  $\mathbf{n}_k$  is due to isotropic ambient noise, and estimate  $\mathbf{R}_{\mathbf{n}}(f)$  independently at each frequency using the approach described in [9]. It is likely that a better estimate of  $\mathbf{R}_{\mathbf{n}}(f)$  may be attained by leveraging knowledge of the frequency dependence of the ambient noise. For example, the noise power may be a slowly varying function of frequency, which would allow some amount of frequency smoothing. However, to facilitate comparisons between the two different source parameter estimation techniques described in Sections IV-B1 and IV-B2, we restrict ourselves to narrowband estimates.

## B. Source Parameter Estimation

We consider source parameter estimation under two scenarios: when the spectral masks  $p_m(f)$  are known and when they are unknown.

1) *Known Spectral Mask*: Provided one has knowledge of the spectral masks  $p_m(f)$  of the  $M + 1$  signals, one can estimate the source powers  $P_m$  and bearings  $\phi_m$  jointly across all frequencies of interest. We consider the maximum likelihood estimates  $\hat{P}_{m'}$  and  $\hat{\phi}_{m'}$  corresponding to the signal power and bearing of the  $m'$ th source. For a given bearing estimate  $\hat{\phi}_{m'}$ , the maximum likelihood estimate  $\hat{P}_{m'}$  for the  $m'$ th source's signal power is

$$\hat{P}_{m'} = \arg \max_{\hat{P}_{m'}} \left\{ \sum_{q=1}^Q -K [\log |\mathbf{R}_{\mathbf{x}}(\hat{\mathbf{s}}, f_q)| + \text{tr} (\mathbf{R}_{\mathbf{x}}^{-1}(\hat{\mathbf{s}}, f_q) \mathbf{C}_{\mathbf{x}}(f_q))] \right\} \quad (14)$$

with the constraint that  $\hat{P}_{m'} \geq 0$  for some  $m' \in \{0, 1, 2, \dots, m\}$ , where  $\hat{\mathbf{s}} = \{\hat{P}_m, \hat{\phi}_m, \hat{\mathbf{R}}_{\mathbf{n}}\}_{m=0}^M$  denotes the current estimate of all state parameters. As shown in the appendix, the estimate  $\hat{P}_{m'}$  that maximizes (14) also solves the scalar equation

$$0 = \sum_{q=1}^Q p_{m'}(f_q) \times \frac{\hat{P}_{m'} p_{m'}(f_q) + \hat{\nu}_{m'}(\hat{\phi}_{m'}, f_q) - \hat{P}_{\text{MVDR}, m'}(\hat{\phi}_{m'}, f_q)}{[\hat{P}_{m'} p_{m'}(f_q) + \hat{\nu}_{m'}(\hat{\phi}_{m'}, f_q)]^2}, \quad (15)$$

where  $\hat{\nu}_{m'}$  and  $\hat{P}_{\text{MVDR}, m'}$ , and  $\hat{\mathbf{w}}_{m'}^H$  are estimates of the noise-plus-interference power, MVDR power, and MVDR weights as defined by (9)-(12) with  $\mathbf{R}_{n+i, m'}(\mathbf{s}, f)$  replaced by its estimate  $\hat{\mathbf{R}}_{n+i, m'}(\hat{\mathbf{s}}, f)$ .

Equation (15) may be used to estimate the signal power  $\hat{P}_{m'}$  given an estimate of the source's bearing  $\hat{\phi}_{m'}$ . Given an estimate of the signal power  $\hat{P}_{m'}$ , the maximum likelihood estimate for the source's bearing  $\hat{\phi}_{m'}$  is

$$\hat{\phi}_{m'} = \arg \max_{\hat{\phi}_{m'}} \left\{ \sum_{q=1}^Q -K [\log |\mathbf{R}_{\mathbf{x}}(\hat{\mathbf{s}}, f_q)| + \text{tr} (\mathbf{R}_{\mathbf{x}}^{-1}(\hat{\mathbf{s}}, f_q) \mathbf{C}_{\mathbf{x}}(f_q))] \right\}, \quad (16)$$

which may be simplified to the following scalar expression:

$$\hat{\phi}_{m'} = \arg \max_{\hat{\phi}_{m'}} \left\{ \sum_{q=1}^Q \left[ -\log \left( 1 + \frac{\hat{P}_{m'} p_{m'}(f_q)}{\hat{\nu}_{m'}(\hat{\phi}_{m'}, f_q)} \right) + \left( \frac{\frac{\hat{P}_{m'} p_{m'}(f_q)}{\hat{\nu}_{m'}(\hat{\phi}_{m'}, f_q)}}{1 + \frac{\hat{P}_{m'} p_{m'}(f_q)}{\hat{\nu}_{m'}(\hat{\phi}_{m'}, f_q)}} \right) \frac{\hat{P}_{\text{MVDR}, m'}(\hat{\phi}_{m'}, f_q)}{\hat{\nu}_{m'}(\hat{\phi}_{m'}, f_q)} \right] \right\}. \quad (17)$$

As in [6], the bearing and power maximum likelihood estimates may be determined by solving (15) for a finely discretized set of  $\hat{\phi}_{m'} \in [0, 2\pi)$ . The resulting set of parameter pairs  $(\hat{\phi}_{m'}, \hat{P}_{m'})$  is then substituted into (17) so as to determine which parameter pair maximizes the log-likelihood ratio and thus constitute the maximum likelihood estimates.

2) *Unknown Spectral Masks*: Lacking *a priori* knowledge of the spectral masks  $p_m(f)$  of the  $M + 1$  signals, one must estimate the *narrowband* signal power  $\sigma_{m, q}^2 = P_m p_m(f_q)$  for each  $q \in \{1, 2, \dots, Q\}$ . From the discussion in Section IV-B1, it is tempting to seek a bearing  $\phi_{m'}$  and a set of narrowband signal powers  $\sigma_{m', q}^2$  for the  $m'$ th signal that maximizes the broadband log-likelihood ratio in (13). However, we have found this approach to be unsatisfactory for Bayesian tracking. This is because the maximum likelihood estimates for the narrowband signal powers  $\hat{\sigma}_{m', q}^2$  always result in a set of frequency-dependent log-likelihood ratios that add constructively at the maximum likelihood estimate for the bearing  $\phi_{m'}$  of the  $m'$ th signal. This likelihood maximization is expected for any maximum likelihood estimate, but here it has the unintended consequence of *always* driving the broadband log-likelihood ratio high enough such that the Bayesian tracker declares a target detection even when no target is present.

Due to this false-detection issue, we investigated a simpler approach to marginalization of the log-likelihood ratio for use when the signals' spectral masks are unknown. In this approach, we treat the measurements at the different frequencies as independent of one another, and independently compute  $Q$  narrowband SSLRs of the form

$$\log L_{m'}(\mathbf{X}(f_q) | \phi_0) = K \left[ -\log \left( 1 + \frac{\sigma_{m', q}^2}{\nu(\phi_{m'}, f_q)} \right) + \left( \frac{\frac{\sigma_{m', q}^2}{\nu(\phi_{m'}, f_q)}}{1 + \frac{\sigma_{m', q}^2}{\nu(\phi_{m'}, f_q)}} \right) \frac{P_{\text{MVDR}, m'}(\phi_{m'}, f_q)}{\nu(\phi_{m'}, f_q)} \right]. \quad (18)$$

This effectively converts the problem of marginalizing a broadband SSLR spanning  $Q$  frequencies into one of marginalizing  $Q$  narrowband SSLRs. Details on marginalizing a narrowband log-likelihood ratio of the form shown in (18) may be found in [6], [8]–[10]. Here, we use the specific estimation procedures described in [9].

### C. Iterative Refinement of Parameter Estimates

Due to the interdependence of the noise and signal parameter estimates, they must be determined iteratively in a manner analogous to the alternating maximization algorithm [6], [10].

For the frequency-independent source parameter estimation described in Section IV-B2, this iterative refinement is done independently for each frequency  $f_q$ . For the spectral mask-based source parameter estimation described in Section IV-B1, the iterative refinement is done as described below.

Following [6], the iterative estimation procedure is initialized by first assuming one source is present ( $M = 0$ ). At each frequency  $f_q$ , the mean of  $N - M - 1$  smallest eigenvalues of  $\mathbf{C}_x(f_q)$  is used as an estimate of the noise power, which leads to an estimate of the noise covariance matrix  $\mathbf{R}_n(f)$ . Then, the signal parameters for the  $M + 1$  sources are estimated. This is followed by a new noise estimate, then a new set of signal parameters, and so on until the estimates converge. The assumed number of sources is then incremented (i.e.,  $M = 1$ ), a new initial noise estimate is computed, and the signal parameter estimates and noise estimates are again iteratively refined. This procedure is repeated until the assumed number of sources equals the actual number of sources, which must be known *a priori* or else postulated from the measurements.

Once all parameters have been determined, the signal-of-interest's direction-of-arrival  $\phi_0$  is treated as an unknown dependent variable so as to evaluate the broadband SSLR in (13) for different bearings of the source-of-interest. This measurement-based likelihood function may then be combined with *a priori* estimates of the probability density function of the source-of-interest's bearing/location and a stochastic model of the source-of-interest's kinematics so as to realize a Bayesian tracker.

## V. SIMULATIONS

The bearing-dependent SSLRs were mapped to Cartesian space for integration into a 2-D Cartesian Bayesian tracker designed to facilitate multi-sensor data fusion. The tracker featured a 2-D Cartesian position-velocity probability density grid [11], a hybrid particle-grid motion update procedure [12], and a birth-death model for the movement of a source into or out of the tracking region [13]. Further details about the Bayesian tracker implementation may be found in [14], [15]. Although the tracker supports multi-sensor data fusion, we limit our scope to single sensor scenarios so as to compare the performance of the tracker with element-level versus CBF-level signals.

The Sonar Simulation Toolset [16] was used to generate three different underwater target detection and tracking scenarios. The simulations used a uniform circular array of  $N = 50$  omnidirectional elements. The inter-element spacing was 0.75 m, which corresponds to a half-wavelength at 1 kHz. The array was positioned in the horizontal plane at a depth of 20 m. Tracking was done within an 80 km by 80 km region centered about the array. The signal of interest was generated by a single target located 54 km east of the array at a depth of 20 m and moving directly toward the array at a constant speed of 5 m/s. The signal generated by the target had a Gaussian power-spectral density centered at  $f_c = 750$  Hz with a root-mean-square (RMS) bandwidth (i.e., "standard deviation") of  $\sigma_{\text{BW}}$ . In the simulations, we considered signal RMS bandwidths of

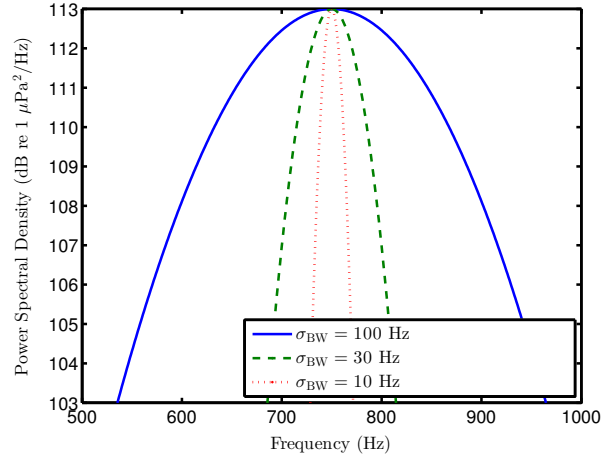


Fig. 1. Signal power spectral densities for different signal bandwidths  $\sigma_{\text{BW}}$ .

TABLE I  
SIMULATION DETAILS

Parameter	Value
Ambient noise spectrum level	60 dB re 1 $\mu\text{Pa}^2/\text{Hz}$
Target peak spectrum level	113 dB re 1 $\mu\text{Pa}^2/\text{Hz}$
Measurement center frequency	750 Hz
Snapshot duration	$T = 0.23$ s
Time snapshots per measurement	$K = 515$
Measurement duration	$KT = 120$ s
FFT resolution	4.3 Hz
Array directivity	16 dB at 750 Hz

$\sigma_{\text{BW}} = \{100, 30, 10\}$  Hz. Figure 1 presents the power spectral densities for the different bandwidths. Additional simulation details are provided in Table I.

We considered four tracking scenarios based on the different source parameter estimation techniques and different degrees of *a priori* knowledge of the signal. These scenarios are outlined in Table II. The 'Tracking Bandwidth' column indicates what portion of the 500 Hz measurement bandwidth was used for broadband tracking; for all scenarios, the tracking bandwidth (BW) was centered about 750 Hz. 'Full BW' indicates that the log-likelihood ratio was evaluated over the entire 500 Hz measurement bandwidth; 'Signal BW' indicates that log-likelihood ratio was evaluated for frequencies within a  $\pm 2\sigma_{\text{BW}}$  band (i.e., plus/minus two standard deviations of the Gaussian mask) centered about 750 Hz.

The 'Signal BW, known  $p_m(f)$ ' scenario evaluates the broadband tracking performance when one has complete *a priori* knowledge of the signal of interest and represents the best-case scenario in terms of both *a priori* knowledge and, as will be shown, tracker performance. The 'Signal BW,  $p_m(f) \approx 1$ ' scenario evaluates the broadband tracking performance when one has *a priori* knowledge of the signal-of-interest's frequency band and approximate albeit erroneous knowledge of its spectral mask. The 'Signal BW, unknown

TABLE II  
TRACKING SCENARIOS

Name	Description	Tracking Bandwidth (BW)	Source Parameter Estimation Technique
Signal BW, known $p_m(f)$	Broadband tracking over the target signal's bandwidth; signal's $f_c$ is known; signal's BW is approximated as $4\sigma_{\text{BW}}$ ; signal's spectral mask is known exactly over approximated BW.	$4\sigma_{\text{BW}}$	Section IV-B1 <i>Known Spectral Mask</i>
Signal BW, $p_m(f) \approx 1$	Broadband tracking over the target signal's bandwidth; signal's $f_c$ is known; signal's BW is approximated as $4\sigma_{\text{BW}}$ ; spectral mask is approximated as constant over approximated BW.	$4\sigma_{\text{BW}}$	Section IV-B1 <i>Known Spectral Mask</i>
Signal BW, unknown $p_m(f)$	Broadband tracking over the target signal's bandwidth; signal's $f_c$ is known; signal's BW is approximated as $4\sigma_{\text{BW}}$ ; spectral mask is unknown.	$4\sigma_{\text{BW}}$	Section IV-B2 <i>Unknown Spectral Mask</i>
Full BW, unknown $p_m(f)$	Broadband tracking over the entire measurement BW; signal's $f_c$ and BW unknown; spectral mask is unknown.	500 Hz (Full BW)	Section IV-B2 <i>Unknown Spectral Mask</i>
Narrowband	Narrowband tracking at 750 Hz.	4.3 Hz (FFT resolution)	Section IV-B2 <i>Unknown Spectral Mask</i>

$p_m(f)$ ' scenario evaluates the broadband tracking performance when one has *a priori* knowledge of the signal-of-interest's frequency band (i.e., center frequency and bandwidth) but no knowledge of its spectral mask. The 'Full BW, unknown  $p_m(f)$ ' scenario evaluates the broadband tracking performance when one has no *a priori* knowledge of the signal emitted by the target. Finally, the 'Narrowband' tracking scenario at the single frequency of 750 Hz provides a reference for gauging the relative performance of the different broadband tracking scenarios.

#### A. Tracker Performance Metrics

We consider three performance metrics for the Bayesian tracker: target probability  $P_t$ , the error in the maximum *a posteriori* (MAP) of the target bearing probability density function (PDF)  $\phi_{\text{MAP}}$ , and the angular spread of the target bearing PDF  $\Lambda_\phi$ . The target probability comes naturally from the Bayesian tracker framework and indicates the probability that a target is in the region of interest. The MAP target bearing is the maximum of the posterior of the target bearing PDF, denoted  $f_\Phi(\phi)$ , which is itself conditioned on a target being in the tracking region. The target bearing PDF  $f_\Phi(\phi)$  is calculated by marginalizing the tracker's 2-D Cartesian target position PDF with respect to range from the array. The bearing PDF angular spread provides a measure of target localization. As shown in [17], it is computed as

$$\Lambda_\phi = \sqrt{1 - \frac{|F_1|^2}{|F_0|^2}}, \quad (19)$$

where  $F_n$  are angular Fourier coefficients calculated as

$$F_n = \int_0^{2\pi} f_\Phi(\phi) e^{jn\phi} d\phi. \quad (20)$$

The bearing PDF angular spread<sup>1</sup> takes on values from 0 to 1, with 0 corresponding to a highly localized target [e.g., for  $f_\Phi(\phi) = \delta(\phi - \phi_0)$  where  $\delta(\phi)$  is the Dirac delta function] and 1 corresponding to a poorly localized target [e.g., for  $f_\Phi(\phi) = 1/(2\pi)$ ].

#### B. Results

Figures 2–4 summarize the tracker's performance for the different tracking scenarios and signal bandwidths. The figures present the average of the performance metrics from the five simulation runs. Figure 2 shows the average target probability. Figure 3 shows the average angular spread of the target bearing PDF. Figure 4 shows the RMS error in the target bearing MAP. We note that at measurements  $\{30, 50, 70\}$ , the target range is  $\{35, 23, 11\}$  km, and the peak spectrum level of the signal of interest arriving at the array is  $\{22, 26, 32\}$  dB re  $1 \mu\text{Pa}^2/\text{Hz}$ , respectively.

For all of the metrics and signal bandwidths, we see that the best performance is achieved with 'Signal BW, known  $p_m(f)$ ', followed closely by 'Signal BW,  $p_m(f) \approx 1$ '. These two scenarios, which rely on exact and approximate knowledge of the signal's spectral mask, respectively, show significant performance gains relative to the other approaches. This clearly demonstrates the utility of approximate knowledge of the signal's spectral mask.

The 'Narrowband' and 'Signal BW, unknown  $p_m(f)$ ' scenarios perform very similarly. Recall that the 'Signal BW, unknown  $p_m(f)$ ' log-likelihood ratio is just the sum of multiple narrowband log-likelihood ratios. This implies that the performance of 'Signal BW, unknown  $p_m(f)$ ' is highly dependent on the underlying tracking performance enabled by the narrowband log-likelihood ratio. By restricting 'Signal BW, unknown  $p_m(f)$ ' to frequencies wherein the power spectral

<sup>1</sup>Angular spread as defined by (19)-(20) was originally conceived as a measure of how incident power is spread in azimuth; that is, the width of a power-angle spectrum. We have found it equally useful for quantifying the width of a bearing-dependent PDF.

density is relatively large, the overall tracking performance of ‘Signal BW, unknown  $p_m(f)$ ’ remains similar to that of the ‘Narrowband’ approach.

Despite this similarity, it is still advantageous to use ‘Signal BW, unknown  $p_m(f)$ ’ over ‘Narrowband’ whenever the signal’s frequency support is known. The broadband log-likelihood ratio used in ‘Signal BW, unknown  $p_m(f)$ ’ inherently sums multiple narrowband log-likelihood ratios at frequencies spanning the signal’s bandwidth. This makes the ‘Signal BW, unknown  $p_m(f)$ ’ approach less sensitive to variations in the signal’s spectral mask as compared to the ‘Narrowband’ approach, which could inadvertently be used at a frequency corresponding to a null in the signal’s spectral mask.

The performance of ‘Full BW, unknown  $p_m(f)$ ’ is comparable to ‘Narrowband’ for  $\sigma_{\text{BW}} = 100$  Hz but is degraded for smaller bandwidths. Recall that ‘Full BW, unknown  $p_m(f)$ ’ uses the entire 500 Hz measurement band and thus uses frequencies outside of the signal’s bandwidth. Narrowband log-likelihood ratios formed at frequencies *outside* of the signal’s bandwidth tend toward a “no target” state that biases the overall broadband likelihood ratio. Going from  $\sigma_{\text{BW}} = 100$  Hz to  $\sigma_{\text{BW}} = 10$  Hz, the signal occupies a shrinking fraction of the overall measurement bandwidth, whereby the “no target” bias increases. This effectively desensitizes the tracker and necessitates an increasingly louder signal (i.e., closer target) in order to detect and localize the target. This exemplifies the difficulties inherent in trying to detect the presence of a signal whose frequency support is unknown and whose bandwidth is much smaller than the overall measurement bandwidth. Ongoing research seeks to develop alternative tracking approaches and/or likelihood ratio formulations that may be used to detect and track a completely unknown signal anywhere within the measurement band.

## VI. CONCLUSIONS

As demonstrated by the simulations, *a priori* knowledge of a broadband signal’s spectral mask enables significant improvement in the detection and localization performance of a Bayesian tracker, even when the knowledge of the signal’s spectral mask is approximate. The results presented here showed a relatively small degradation in performance when going from the exact spectral mask to an approximate one. Further research is necessary to better understand how far the approximate spectral mask may deviate from the actual spectral mask and still provide satisfactory tracking performance. For scenarios where both the signal’s spectral mask and its total power may be approximated, the broadband tracking approach described here may be combined with the source level modeling technique described in [14] so as to yield both bearing and range estimates for sources emitting broadband signals. This would essentially enable leveraging of another layer of *a priori* knowledge of the signal.

In cases where the signal’s spectral mask cannot be approximated but the signal’s frequency range is known, the performance of the broadband tracking approach presented here was

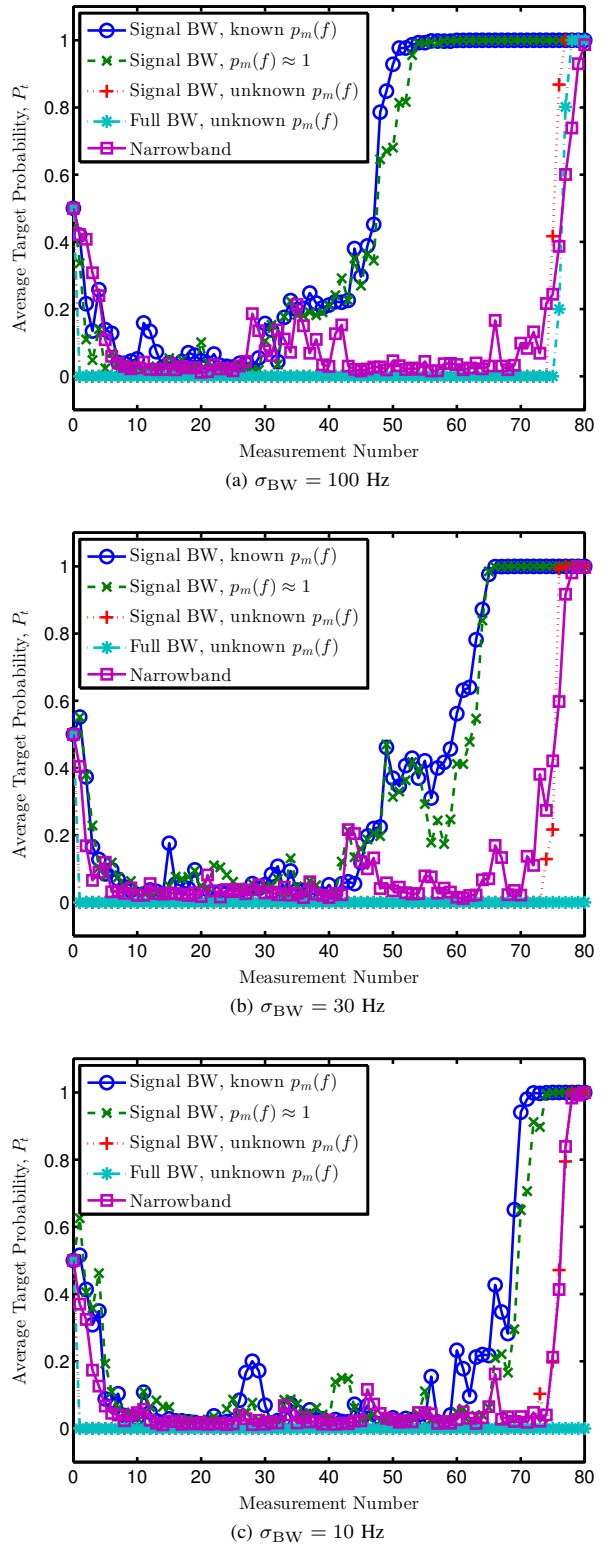


Fig. 2. Target probability averaged over the five simulation runs for different signal bandwidths  $\sigma_{\text{BW}}$ .

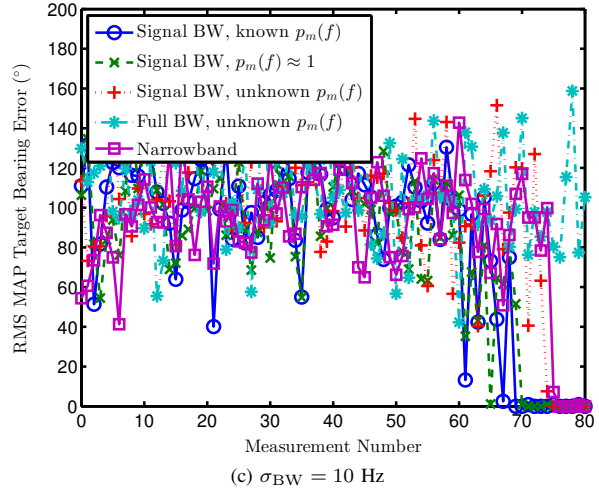
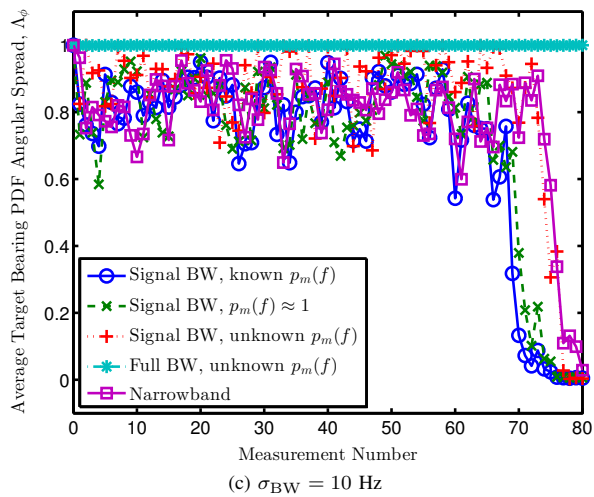
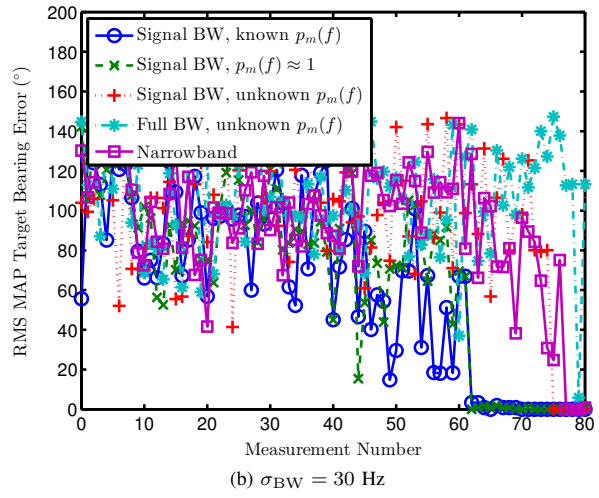
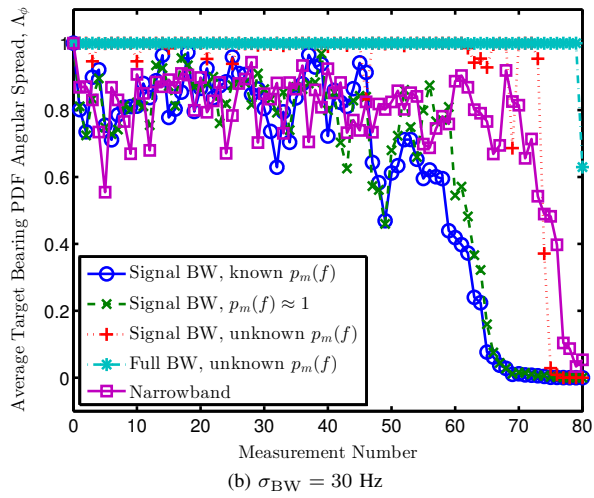
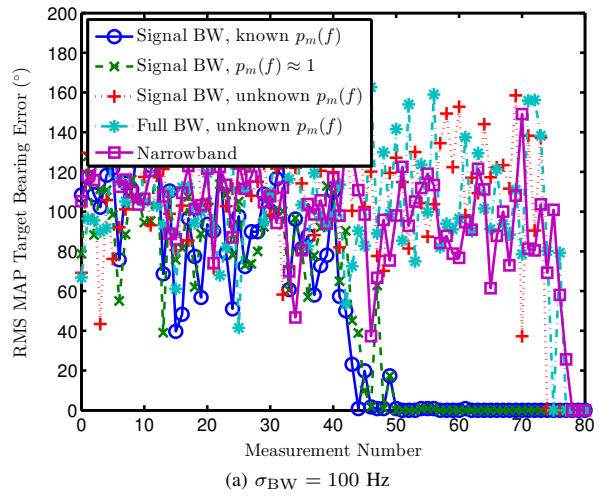
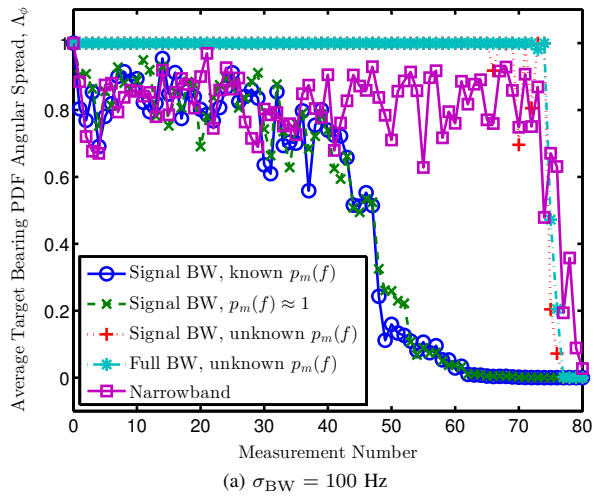


Fig. 3. Target bearing angular spread averaged over the five simulation runs for different signal bandwidths  $\sigma_{\text{BW}}$ .

Fig. 4. Target bearing MAP error magnitude averaged over the five simulation runs for different signal bandwidths  $\sigma_{\text{BW}}$ .

comparable to that of a narrowband tracker operating at the frequency corresponding to the signal's peak power spectral density. This implies that the broadband tracking approach provided robustness to the frequency-dependent variability of the signal's actual spectral mask. Finally, we presented a broadband tracking approach that is applicable even when both the signal's spectral mask and its frequency range are unknown. However, the lack of knowledge of the signal can significantly impair tracking performance, particularly if the signal's bandwidth is a small fraction of the overall measurement band. Improving the broadband tracking performance in the absence of signal knowledge is a focus of ongoing research efforts.

#### APPENDIX

The maximum of (14) may be determined by taking its derivative with respect to  $\hat{P}_{m'}$  and setting it to zero:

$$\frac{\partial}{\partial \hat{P}_{m'}} \sum_{q=1}^Q -K [\log |\mathbf{R}_{\mathbf{x}}(\hat{\mathbf{s}}, f_q)| + \text{tr}(\mathbf{R}_{\mathbf{x}}^{-1}(\hat{\mathbf{s}}, f_q) \mathbf{C}_{\mathbf{x}}(f_q))] = 0. \quad (21)$$

Equation (21) simplifies to

$$\sum_{q=1}^Q p_{m'}(f_q) \text{tr}([\mathbf{R}_{\mathbf{x}}^{-1}(\hat{\mathbf{s}}, f_q) - \mathbf{R}_{\mathbf{x}}^{-1}(\hat{\mathbf{s}}, f) \mathbf{C}_{\mathbf{x}}(f_q) \mathbf{R}_{\mathbf{x}}^{-1}(\hat{\mathbf{s}}, f_q)] \times \mathbf{v}(\hat{\phi}_{m'}, f_q) \mathbf{v}^H(\hat{\phi}_{m'}, f_q)) = 0. \quad (22)$$

By use of the circularity of the matrix trace operator, we may move  $\mathbf{v}^H$  to the left side of the matrix trace argument. This collapses the matrix argument to a scalar, which allows removal of the trace operator. Then, by use of the identity  $\mathbf{R}_{\mathbf{x}}^{-1} = \mathbf{R}_{\mathbf{x}}^{-1} \mathbf{R}_{\mathbf{x}} \mathbf{R}_{\mathbf{x}}^{-1}$ , (22) becomes

$$\sum_{q=1}^Q p_{m'}(f_q) \mathbf{v}^H(\hat{\phi}_{m'}, f_q) \mathbf{R}_{\mathbf{x}}^{-1}(\hat{\mathbf{s}}, f_q) \times [\mathbf{R}_{\mathbf{x}}(\hat{\mathbf{s}}, f_q) - \mathbf{C}_{\mathbf{x}}(f_q)] \mathbf{R}_{\mathbf{x}}^{-1}(\hat{\mathbf{s}}, f_q) \mathbf{v}(\hat{\phi}_{m'}, f_q) = 0. \quad (23)$$

Substituting the expression (c.f., [6], [8], [10])

$$\mathbf{R}_{\mathbf{x}}^{-1}(\hat{\mathbf{s}}, f) = \mathbf{R}_{n+i, m'}^{-1}(\hat{\mathbf{s}}, f) - \frac{\hat{P}_{m'} p_{m'}(f) \mathbf{R}_{n+i, m'}^{-1}(\hat{\mathbf{s}}, f) \mathbf{v}(\hat{\phi}_{m'}, f) \mathbf{v}^H(\hat{\phi}_{m'}, f) \mathbf{R}_{n+i, m'}^{-1}(\hat{\mathbf{s}}, f)}{1 + \hat{P}_{m'} p_{m'}(f) \mathbf{v}^H(\hat{\phi}_{m'}, f) \mathbf{R}_{n+i, m'}^{-1}(\hat{\mathbf{s}}, f) \mathbf{v}(\hat{\phi}_{m'}, f)} \quad (24)$$

into (23) and simplifying yields

$$\sum_{q=1}^Q p_{m'}(f_q) \mathbf{v}^H(\hat{\phi}_{m'}, f_q) \mathbf{R}_{n+i, m'}^{-1}(\hat{\mathbf{s}}, f_q) \times [\mathbf{R}_{\mathbf{x}}(\hat{\mathbf{s}}, f_q) - \mathbf{C}_{\mathbf{x}}(f_q)] \mathbf{R}_{n+i, m'}^{-1}(\hat{\mathbf{s}}, f_q) \mathbf{v}(\hat{\phi}_{m'}) \div \left[ \hat{P}_{m'} p_{m'}(f_q) \mathbf{v}^H(\hat{\phi}_{m'}, f_q) \mathbf{R}_{n+i, m'}^{-1}(\hat{\mathbf{s}}, f_q) \mathbf{v}(\hat{\phi}_{m'}, f_q) + 1 \right]^2 = 0. \quad (25)$$

By dividing the numerator and denominator in (25) by  $\left[ \mathbf{v}^H(\hat{\phi}_{m'}, f_q) \mathbf{R}_{n+i, m'}^{-1}(\hat{\mathbf{s}}, f_q) \mathbf{v}(\hat{\phi}_{m'}, f_q) \right]^2$  and making use of (5) and (11), (25) becomes

$$\sum_{q=1}^Q p_{m'}(f_q) \left( \hat{P}_{m'} p_{m'}(f_q) + \hat{\mathbf{w}}^H(\hat{\phi}_{m'}, f_q) [\mathbf{R}_{n+i, m'}(\hat{\mathbf{s}}, f_q) - \mathbf{C}_{\mathbf{x}}(f_q)] \hat{\mathbf{w}}(\hat{\phi}_{m'}, f_q) \right) \div \left[ \hat{P}_{m'} p_{m'}(f_q) + \hat{\mathbf{w}}^H(\hat{\phi}_{m'}, f_q) \mathbf{R}_{n+i, m'}(\hat{\mathbf{s}}, f_q) \hat{\mathbf{w}}(\hat{\phi}_{m'}, f_q) \right]^2 = 0. \quad (26)$$

Substitution of (10) and (9) into (26) yields the expression in (15).

#### ACKNOWLEDGMENT

This work was supported by the Office of Naval Research under contract no. N00014-11-G-0041-19.

#### REFERENCES

- [1] R. E. Zarnich, "A fresh look at 'broadband' passive sonar processing," in *Proc. of the ASAP Workshop*, vol. 1, 10–11 March 1999.
- [2] M. Bono, B. Shapo, P. McCarty, and R. Bethel, "Subband energy detection in passive array processing," in *Proc. ASAP Workshop*, vol. 2, 13–14 March 2001, pp. 25–30.
- [3] B. Shapo and R. Bethel, "An overview of the probability density function (PDF) tracker," in *OCEANS 2006*, 18–21 September 2006, pp. 1–6.
- [4] C. Kreucher and B. Shapo, "Multitarget detection and tracking using multisensor passive acoustic data," *IEEE J. Ocean. Eng.*, vol. 36, no. 2, pp. 205–218, April 2011.
- [5] R. E. Bethel and K. L. Bell, "A MLE approach to joint array detection and direction of arrival estimation," in *Proc. Sensor Array and Multichannel Signal Processing Workshop*, 4–6 August 2002, pp. 169–173.
- [6] B. A. Yocom, B. R. La Cour, and T. W. Yudichak, "A Bayesian approach to passive sonar detection and tracking in the presence of interferers," *IEEE J. Ocean. Eng.*, vol. 36, no. 3, pp. 386–405, July 2011.
- [7] K. L. Bell, R. E. Zarnich, and R. Wasyk, "MAP-PF wideband multitarget and colored noise tracking," in *IEEE Int. Conf. Acoustics Speech and Signal Processing*, 14–19 March 2010, pp. 2710–2713.
- [8] B. A. Yocom, "Bayesian passive sonar tracking in the context of active-passive data fusion," Master's thesis, The University of Texas at Austin, August 2009.
- [9] R. J. Pirkil and J. M. Aughenbaugh, "Bayesian passive sonar tracking with conventional beamformer-level data," in *Information Fusion, 18th Int. Conf. on*, 6–9 July 2015, accepted.
- [10] R. E. Bethel, "Joint detection and estimation in a multiple signal array processing environment," Ph.D. dissertation, George Mason University, 2002.
- [11] J. M. Aughenbaugh and B. R. La Cour, "Measurement-guided likelihood sampling for grid-based Bayesian tracking," *J. Adv. Inf. Fusion*, vol. 5, no. 2, pp. 108–127, 2010.
- [12] —, "Particle-inspired motion updates for grid-based Bayesian trackers," in *Information Fusion, 14th Int. Conf. on*, 5–8 July 2011, pp. 1–8.
- [13] B. R. La Cour, "Stationary priors for Bayesian target tracking," in *Information Fusion, 11th Int. Conf. on*, 30 June–3 July 2008, pp. 1–6.
- [14] B. A. Yocom, J. M. Aughenbaugh, and B. R. La Cour, "Range-sensitive Bayesian passive sonar tracking," in *Information Fusion, 13th Int. Conf. on*, 26–29 July 2010, pp. 1–10.
- [15] J. M. Aughenbaugh and B. R. La Cour, "Computationally efficient Bayesian tracking," in *SPIE Defense, Security, and Sensing*, 25–26 April 2012.
- [16] R. P. Goddard, "The Sonar Simulation Toolset, Release 4.6: Science, Mathematics, and Algorithms," Applied Physics Laboratory, University of Washington, Tech. Rep. APL-UW TR 0702, October 2008.
- [17] G. D. Durgin and T. S. Rappaport, "Basic relationship between multipath angular spread and narrowband fading in wireless channels," *Electronics Letters*, vol. 34, no. 25, pp. 2431–2432, December 1998.